Optical critical points of thin-film $Ge_{1-y}Sn_y$ alloys: A comparative $Ge_{1-y}Sn_y/Ge_{1-x}Si_x$ study

Vijay R. D'Costa,[1] Candi S. Cook,[1,2] A. G. Birdwell,[3] Chris L. Littler,[4] Michael Canonico,[5] Stefan Zollner,[6] John Kouvetakis,[2] and José Menéndez[1]

[1]*Department of Physics and Astronomy, Arizona State University, Tempe, Arizona 85287-1504, USA*

[2]*Department of Chemistry and Biochemistry, Arizona State University, Tempe, Arizona 85287-1604, USA*

[3]*Semiconductor Electronics Division, National Institute of Standards and Technology, Gaithersburg, Maryland 20899-8121, USA*

[4]*Department of Physics, University of North Texas, Denton, Texas 76203, USA*

[5]*Freescale Semiconductor, Physical Analysis Lab Arizona (PALAZ), 2100 E. Elliot Road, Tempe, Arizona 85284, USA*

[6]*Freescale Semiconductor, APRDL, MD K10, 3501 Ed Bluestein Boulevard, Austin, Texas 78721, USA*

(Received 6 October 2005; revised manuscript received 11 January 2006; published 31 March 2006)

The E_0, $E_0+\Delta_0$, E_1, $E_1+\Delta_1$, E_0', and E_2 optical transitions have been measured in $Ge_{1-y}Sn_y$ alloys ($y<0.2$) using spectroscopic ellipsometry and photoreflectance. The results indicate a strong nonlinearity (bowing) in the compositional dependence of these quantities. Such behavior is not predicted by electronic structure calculations within the virtual crystal approximation. The bowing parameters for $Ge_{1-y}Sn_y$ alloys show an intriguing correlation with the corresponding bowing parameters in the $Ge_{1-x}Si_x$ system, suggesting a scaling behavior for the electronic properties that is the analog of the scaling behavior found earlier for the vibrational properties. A direct consequence of this scaling behavior is a significant reduction (relative to prior theoretical estimates within the virtual crystal approximation) of the concentration y_c for a crossover from an indirect- to a direct-gap system.

DOI: 10.1103/PhysRevB.73.125207 PACS number(s): 71.22.+i, 78.20.−e, 78.40.−q

I. INTRODUCTION

Since the discovery that the diamond-structure semimetal α-Sn can be grown by Molecular Beam Epitaxy (MBE) on nearly lattice-matched InSb and CdTe substrates,[1] there has been considerable interest in semiconductor compounds containing Sn. The original approach of Farrow and co-workers was later extended to $Ge_{1-y}Sn_y$ alloys using substrates that minimize the expected lattice mismatch at different alloy compositions.[2–8] While these experiments were based on the MBE method, crystalline $Ge_{1-y}Sn_y$ alloys have also been grown using other techniques, such as sputtering.[9–11] Recently, advances in chemical vapor deposition (CVD) have made it possible to grow not only binary but also ternary group-IV semiconductor alloys incorporating Sn.[12–16] These CVD materials can be deposited directly on Si substrates. Their large lattice mismatch with Si is fully relieved by misfit dislocations that do not propagate into the films and thus do not deteriorate their physical properties. $Ge_{1-y}Sn_y$ and $Ge_{1-x-y}Si_xSn_y$ alloys with lattice constants as large as 5.83 Å have already been demonstrated. These films represent an intriguing alternative to compositionally graded $Ge_{1-x}Si_x$ alloys as templates for the growth of strain-free $Ge_{1-x}Si_x$ alloys, and they can also act as templates for the deposition of *III-V* semiconductors on Si.

In addition to their attractive structural properties and their potential as templates, $Ge_{1-y}Sn_y$ alloys possess intriguing electronic properties. In this paper, we focus on a crucial aspect of these properties, namely the compositional dependence of optical transition energies and other critical point parameters as measured with infrared and visible spectroscopic ellipsometry and with photoreflectance.

Most earlier studies of the electronic structure of $Ge_{1-y}Sn_y$ alloys focus on the fundamental band gap region in samples grown by Molecular Beam Epitaxy (MBE) or sputtering on Ge substrates or Ge buffer layers on Si (Refs. 17–19). There is also a report of higher-energy transitions in polycrystalline films grown by sputtering.[9] The present work covers both the band gap region and higher interband transitions. We have measured the compositional dependence not only for the transition energies, but also for other parameters such as critical point broadenings and amplitudes, which can provide deeper insight into the electronic structure of these systems. Preliminary ellipsometric work on $Ge_{1-y}Sn_y$ alloys appeared in Refs. 13, 14, and 20. $Ge_{1-y}Sn_y$ alloy samples grown by CVD have a high degree of structural quality, and we believe that these structural improvements manifest themselves in the optical properties of our layers: whereas previous workers invoked transitions between localized states to explain their optical absorption measurements,[17–19] the optical data presented here can be understood in terms of a Ge-like band structure.

The optical response of semiconductors shows several characteristic features at transition energies E_i that can be associated with critical points in the joint valence-conduction density of electronic states.[21] In most alloy semiconductors the energies $E_i(x)$ of the critical point features are found to have a smooth compositional dependence that can be well described by a quadratic polynomial of the form

$$E_i(x) = E_i^A x + E_i^B(1-x) - b_i x(1-x), \tag{1}$$

where A and B refer to the two crystalline semiconductor systems being alloyed. The coefficient b_i is called the bowing parameter. Knowledge of the bowing parameter is very important for applications, particularly when the transition in question corresponds to the lowest-energy gap. This interest has fueled intense research efforts to measure bowing parameters and understand their microscopic origin.

The mere fact that critical point structures are observed in the optical response of alloy semiconductors suggests that these materials can be described in terms of an average perfect crystal. Such a crystal can be thought of as made of fictitious atoms that generate a potential given by a compositionally weighted average of the corresponding potentials in the parent semiconductors' atoms. This is the so-called Virtual Crystal Approximation (VCA). The application of the VCA to semiconductors has been reviewed by Jaros.[22] Due to the nonlinear nature of the eigenvalue problem, the VCA can lead to bowing in the compositional dependence of band gaps even if the potential interpolation is exactly linear in the alloy composition. Unfortunately, the agreement with experiment is not always good,[22] and it has been argued[23] that the bowing values obtained within the VCA are not even unique. In the case of $Ge_{1-y}Sn_y$ alloys, VCA calculations using a tight-binding approach[24] predict $b=0.30$ eV for the lowest direct gap, whereas VCA calculations within a pseudopotential formalism lead to $b=-0.40$ eV for the same transition.[25] The two calculations do not even agree on the sign of the bowing, and their predicted bowing magnitudes are much smaller than $b=2.8$ eV, the experimental value reported by He and Atwater.[17] This indicates that $Ge_{1-y}Sn_y$ alloys cannot be understood within the VCA. By contrast, the VCA is a good approximation for $Ge_{1-x}Si_x$ alloys.[26–28] The calculated optical transition energies are roughly linear with composition, in good agreement with experiments, which show a small bowing.[29–32] However, it is important to stress that even in cases in which the compositional dependence of optical transition energies are predicted correctly, the VCA does not account for the considerable alloy broadening observed in interband transitions.

Electronic structure features that cannot be explained within the VCA are often dubbed as "disorder effects." A possible way of including these effects in a theoretical treatment is the so-called Coherent Potential Approximation (CPA). (For a review of early CPA work on semiconductors, see Ref. 22.) The CPA has been applied to $Ge_{1-x}Si_x$ alloys with considerable success:[26,27] it predicts a moderate bowing in the optical transition energies, and it predicts the values of broadening that appear to be in good agreement with the electroreflectance data of Kline *et al.*[29] (However, more recent ellipsometric work suggests that the experimental broadenings are considerably larger than those calculated within the CPA.[32,33]) We are not aware of any CPA calculations for $Ge_{1-y}Sn_y$ alloys.

Even though the use of the VCA as an initial approximation and the subsequent incorporation of disorder effects via the CPA represent an attractive conceptual framework to analyze the experimental optical properties of semiconductor alloys, the nature of the relevant alloy disorder suggests a different point of view. The electronic properties of semiconductors are mainly determined by interactions between near-neighbor atoms, and therefore the properties of alloy semiconductors result from the contribution of a handful of possible local atomic configurations. Such local configurations lead to bond distortions that are far from random. Structural models of alloys incorporate these features from the outset. In practice, these models are implemented by considering small, periodic structures that preserve the chemical identity of the elements and reproduce the main structural features of the alloy. The alloy properties are then computed by either averaging over selected structures,[23,34] or by designing "Special Quasirandom Structures" that mimic the first few alloy correlation functions in such a way that they represent the closest periodic analog to the random alloy.[35,36] An extreme example of this approach applied to $Ge_{1-x}Si_x$ alloys is the work of Tekia *et al.* (Ref. 37) who calculate the direct gap bowing by interpolating between Si, Ge and a zincblende-structure SiGe. They find $b=0.23$ eV, in good agreement with experiment. If we apply the same procedure to $Ge_{1-y}Sn_y$ alloys, using a calculated band structure for zinc-blende SnGe,[38] we find $b=0.58$ eV, which is still in disagreement with experiment but is better than any of the VCA predictions. A more refined calculation by Chibane *et al.*,[39] using eight-atom supercells, predict a large and compositional-dependent positive bowing for the direct gap in $Ge_{1-y}Sn_y$alloys, in good agreement with the experimental values reported thus far.[14,17]

The previous observation of a large bowing for the direct band gap[14,17] and the prediction of a compositional-dependent bowing[39] suggest that $Ge_{1-y}Sn_y$ alloys might fall in the "giant bowing" regime discussed by Wei and Zunger.[40] This is the case in $Si_{1-z}C_z$ and $Ge_{1-x-z}Si_xC_z$ alloys, where the band gap has been shown to *decrease* as a function of the C-concentration z for small values of z.[41–43] The physics of giant bowing appears to be related to the formation of deep levels as a result of the large mismatch of atomic level eigenvalues between the "impurity" and the host. According to Harrison,[44] the *s*-function eigenvalues are −19.38, −14.79, −15.16, and −13.04 eV for C, Si, Ge, and Sn, respectively. The corresponding *p*-function eigenvalues are −11.07, −7.59, −7.33, and −6.76 eV, respectively. Since the Ge-Sn differences are much smaller than the Si-C differences, we expect $Ge_{1-x}Si_x$ alloys to provide a better conceptual framework than $Si_{1-z}C_z$ alloys for the understanding of the electronic structure of $Ge_{1-y}Sn_y$ alloys. The detailed experimental study presented here confirms that the electronic structure of $Ge_{1-y}Sn_y$ alloys is indeed more $Ge_{1-x}Si_x$-like than $Si_{1-z}C_z$-like. We find larger bowing parameters in $Ge_{1-x}Sn_x$ than in $Ge_{1-x}Si_x$, but these parameters do not reach the extraordinarily large values reported for systems such as GaN_xAs_{1-x} (Ref. 45). Moreover, we find that the bowing parameters in $Ge_{1-y}Sn_y$ alloys and $Ge_{1-x}Si_x$ alloys are approximately proportional to the product of the atomic size mismatch and the electronegativity difference. This is the electronic-structure analog to the remarkable scaling correlation we have found for the compositional dependence of Raman frequencies in the two systems.[46]

II. EXPERIMENT

A. Samples

Our $Ge_{1-y}Sn_y$ samples were grown by ultrahigh vacuum CVD on Si (100) substrates using a deuterium-stabilized Sn hydride with digermane.[12,14,16] We prepared samples with composition $0.02 \leqslant y \leqslant 0.20$ and thickness $50\ \text{nm} \leqslant t \leqslant 200$ nm, respectively. Figure 1 summarizes the structural characterization analysis for a typical $Ge_{1-y}Sn_y$ film. The

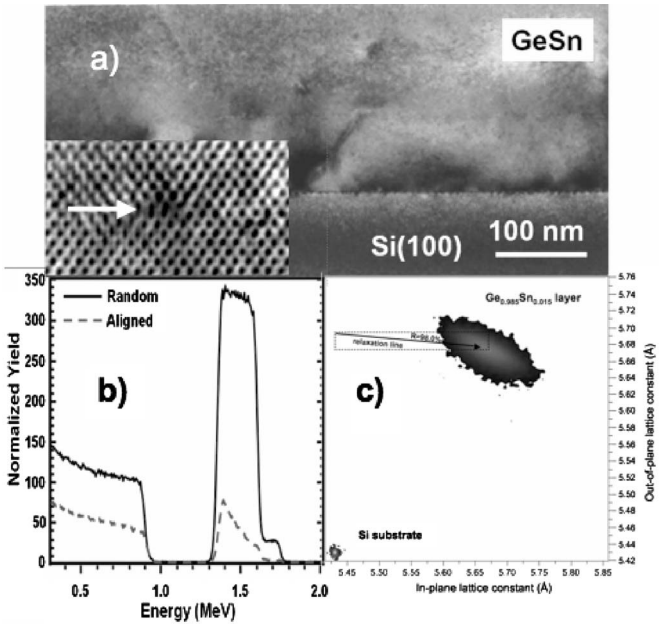

FIG. 1. (a) Diffraction contrast XTEM micrograph of a $Ge_{0.96}Sn_{0.04}$ film grown on Si(100). The inset shows a high resolution view of the interface and the location of a Lomer defect (arrow). (b) RBS random and aligned spectra of a 200 nm $Ge_{0.96}Sn_{0.04}$ film grown on Si(100). The high degree of channeling indicates a monocrystalline and perfectly epitaxial layer. The ratio of the aligned versus random peak heights is the same for both elements, indicating complete substitutionality of Sn in the structure. (c) Direct space map showing the in-plane and out-of-plane lattice constants of a $Ge_{0.985}Sn_{0.015}$ layer grown directly on Si. The analysis reveals $a_{par}=5.688$ Å and $a_{perp}=5.676$ Å, so that the residual mismatch strain is about −0.09%.

composition y and thickness t of the films were established by Rutherford backscattering (RBS). The ratio between the aligned and random peak heights in the RBS spectra, which measures the degree of channeling of the incoming He^{2+}ions, is the same for both Ge and Sn. This indicates that the entire Sn content occupies substitutional sites in the average diamond cubic structure. Transmission electron microscopy (TEM) studies confirm the RBS-thicknesses and show that the bulk of the films are virtually dislocation-free. The lattice mismatch between $Ge_{1-y}Sn_y$ and the Si substrate is accommodated by Lomer dislocations at the interface. High-resolution x-ray diffraction reveals single-phase crystalline films. Reciprocal lattice maps indicate that the samples are essentially relaxed, with a residual strain less than 0.1% (compared with about 4% for a fully strained film on Si). The lattice constant as a function of composition can be written as $a(y)=a_{Sn}y+a_{Ge}(1-y)-by(1-y)$, with -0.17 Å$<b<0$ Å. The bowing coefficient for the lattice constant has the opposite sign to that for $Ge_{1-x}Si_x$ alloys ($b=0.026$ Å).[47] This interesting difference between the two systems has been predicted theoretically,[39,48] and shown to be correlated with the behavior of bond lengths in simple molecules containing bonds between group-IV elements.[48]

B. Ellipsometric measurements

The optical properties of the films and a reference Ge sample were investigated at room temperature using a Variable-Angle Spectroscopic Ellipsometer (VASE[49]) with a computer-controlled compensator, and an Infrared Variable Angle Spectroscopic Ellipsometer[50] with a rotating compensator.

Using the visible-UV instrument, the dielectric function of our films was determined from 0.74 to 6.6 eV with 0.01 eV steps from measurements at three angles of incidence (65°, 70°, and 75°). Our monochromator uses three gratings and low-pass optical filters for wavelength selection. The accuracy of the photon energies was tested with a calibration lamp and found to be better than 1 meV.

The IR-VASE system is based on a Fourier-Transform Infrared Spectrometer. It covers the 0.03 to 0.83 eV range. For two samples with $y=0.02$ and $y=0.14$, respectively, the measurements were performed at two angles of incidence: 65° and 75°. Three angles of incidence between 65° and 75° were used for all other samples.

C. Ellipsometric data processing

The ellipsometric data were analyzed in terms of a three-layer model consisting of a Si substrate, a $Ge_{1-y}Sn_y$ alloy, and a surface layer. The known dielectric function $\varepsilon=\varepsilon_1+i\varepsilon_2$ of the Si substrate as well as the native germanium dioxide[51] were used in either tabulated or parametrized form. The dielectric function of the $Ge_{1-y}Sn_y$ alloy was described with a "parametric optical constant model" developed by Johs and Herzinger.[52] The Johs-Herzinger model is related to a lineshape model proposed by Kim and Garland for the dielectric function of zincblende semiconductors.[53] It provides an excellent description of the known dielectric functions of tetrahedral semiconductors using a large number of parameters (typically more than 50 for each material). One of the advantages of using parametric models is that they guarantee Kramers-Kronig consistency between the real and imaginary parts of the dielectric function.

The adjustable parameters of our model are the oxide layer thickness, the $Ge_{1-y}Sn_y$ thickness, and all the parameters of the Johs-Herzinger model that describes the dielectric function of $Ge_{1-y}Sn_y$. They are optimized using a proprietary Marquardt-Levenberg algorithm provided by the ellipsometer's manufacturer. Given the large number of adjustable parameters, a well-converged and physically reasonable fit requires a judicious choice of the initial seed values and the sequential release of the fitting parameters. We start by setting the parameters of the Johs-Herzinger model to values that fit the known dielectric function of pure Ge. Using this ansatz we determine the thicknesses of the native oxide and $Ge_{1-y}Sn_y$ layers. There is very little correlation between the two thickness parameters because the oxide layer thickness affects the results at high photon energies, whereas the $Ge_{1-y}Sn_y$ thickness becomes relevant at those lower photon energies for which the $Ge_{1-y}Sn_y$ layer is partially transparent. The alloy thicknesses obtained at this stage are normally very close to the RBS or TEM values. Next, we allow the parameters of the Johs-Herzinger model to vary

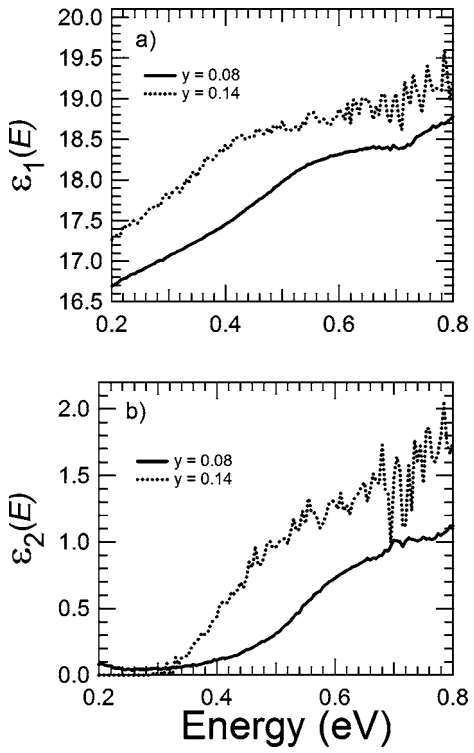

FIG. 2. Infrared real (a) and imaginary (b) parts of the dielectric function of two $Ge_{1-y}Sn_y$ samples.

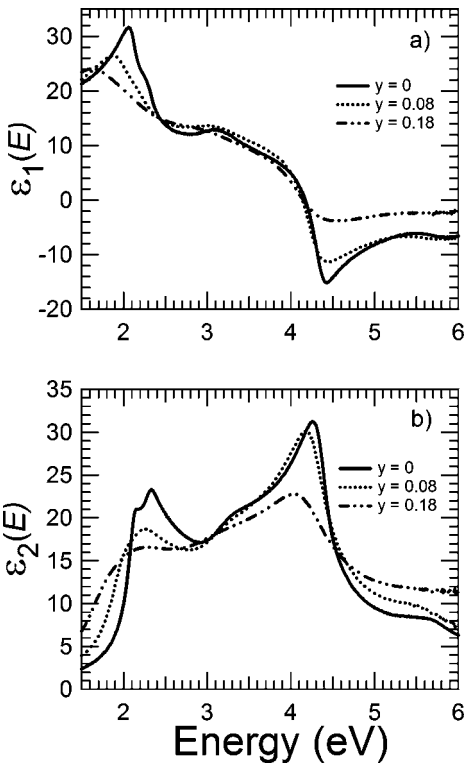

FIG. 3. Visible real (a) and imaginary (b) parts of the dielectric function of two $Ge_{1-y}Sn_y$ samples.

using the layer thicknesses obtained in the previous step. This is usually done by releasing parameters sequentially, starting with those affecting the optical response at high photon energies. Finally, we release all parameters in the model, including thicknesses, and determine simultaneously the native oxide thickness, the $Ge_{1-y}Sn_y$ thickness, and the dielectric function of the alloy.

Systematic errors in the dielectric function of $Ge_{1-y}Sn_y$ determined with this procedure can arise from the assumptions made about the optical properties of the surface layer, from the built-in bias of the Johs-Herzinger description, and from lateral and vertical nonuniformities in the alloy that are not included in the model. The latter, however, are not expected to be very significant, since we find no evidence of nonuniformities from any of our structural studies.

Critical point information for $Ge_{1-y}Sn_y$ can, in principle, be extracted from the fit parameters of the Johs-Herzinger model, but the reliability and meaning of this information is difficult to establish. This is because not all model parameters have a simple physical interpretation that can be linked to specific features of the electronic band structure. On the other hand, it is well-known in optical spectroscopy[54] that critical point contributions can be enhanced by studying derivatives of the dielectric function. The differentiation of the dielectric function suppresses the contributions from slowly varying regions and yields sharp features that can often be fit one at a time with a physically meaningful critical point model containing three of four parameters. Unfortunately, possible small discrepancies between the actual dielectric function and its parametrized Johs-Herzinger version can be highly magnified when comparing second or third derivatives. Therefore, instead of differentiating the parametrized dielectric function, we differentiate a dielectric function obtained without assuming any particular dispersion model. This is done by keeping the layer thicknesses at the values determined from our last fit using the Johs-Herzinger lineshape, and using the values of the ε_1 and ε_2 of $Ge_{1-y}Sn_y$ at each photon energy as the two adjustable parameters in a fit to the multiple-angle ellipsometric data at that particular photon energy. This can be done consecutively, i.e., one photon energy at a time using the previous step value as the starting point (the so-called point-by-point fit) or by fitting all energies simultaneously with the values from the Johs-Herzinger fit as the starting point. In general, these techniques yield the same final values for the dielectric function. The final nonparametric dielectric function turns out to be very close to the Johs-Herzinger lineshape, and therefore it is Kramers-Kronig consistent. This method does not always succeed because of numerical instabilities or thickness variations across the sample.

Nonparametric dielectric functions obtained using the procedure described above are shown in Fig. 2 for the infrared range and Fig. 3 for the visible range. These dielectric functions, with some exceptions to be explained below, are then used for a critical-point analysis using derivatives.

D. Critical point analysis

The real and imaginary parts of the dielectric function—obtained at 0.01 eV intervals—were numerically differentiated and smoothed using corrected Savitzky-Golay coefficients for second-order derivatives with a polynomial of

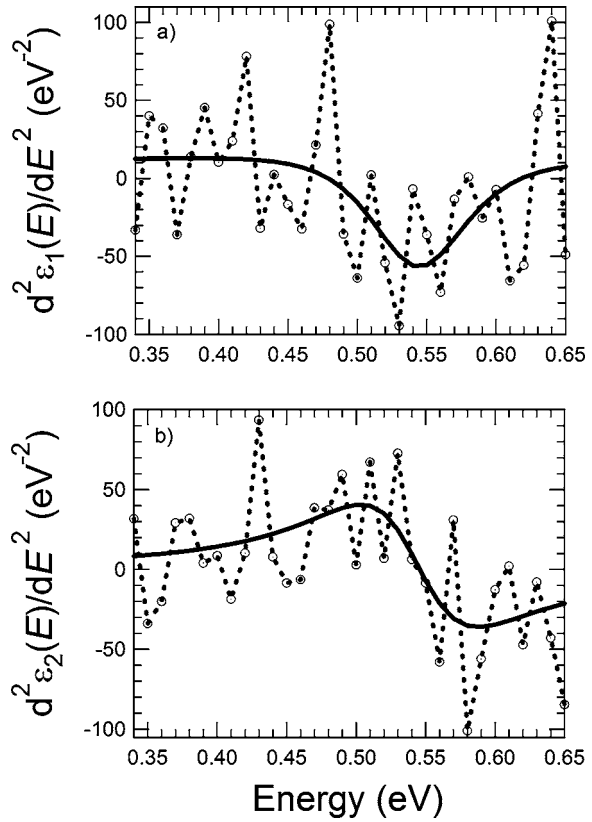

FIG. 4. Numerical second derivative of the point-by-point infrared dielectric function of a $Sn_{0.08}Ge_{0.92}$ sample: (a) real part; (b) imaginary part. The solid line represents a fit with Eq. (2).

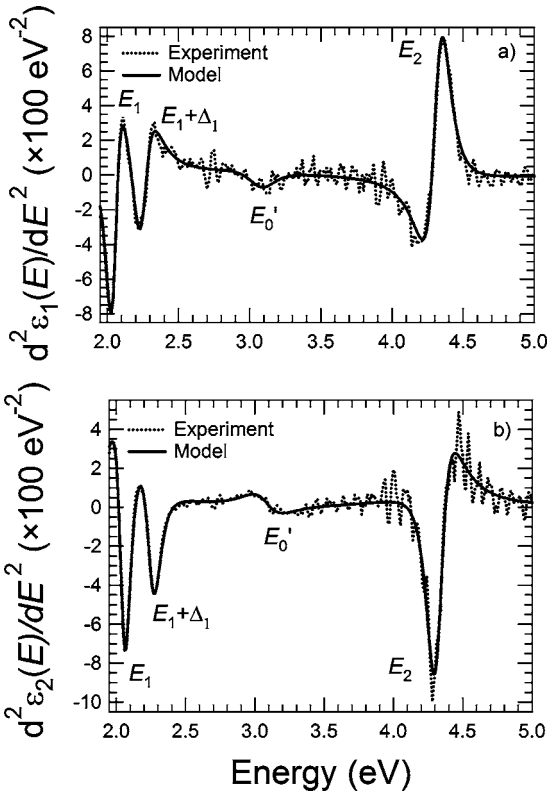

FIG. 5. Numerical second derivative of the point-by-point visible dielectric function of a $Ge_{0.98}Sn_{0.02}$ sample: (a) real part; (b) imaginary part. The solid line represents a fit with Eq. (3).

degree 5.[55,56] The number of smoothing coefficients was optimized via a systematic study in which we compared unsmoothed but differentiated data with smoothed and differentiated data as a function of the number of smoothing coefficients. In the visible range, a choice of 13 smoothing coefficients was found to give a good signal to noise ratio without distorting the lineshape. In the infrared range, we used seven smoothing coefficients.

Figures 4 and 5 show examples of the resulting lineshapes after differentiation for the infrared and visible spectral ranges, respectively. Five well-defined transitions are observed. By analogy with Ge, the infrared transition is assigned to the direct band gap E_0, whereas the visible transitions are assigned to the so-called E_1, $E_1+\Delta_1$, E_0', $E_0'+\Delta_0'$, and E_2 critical points. The relationship between these transitions and the band structure has been discussed in detail by Viña *et al.*[57] Briefly, the direct gap E_0 is located at the center of the diamond structure Brillouin zone (Γ point). The E_1 and $E_1+\Delta_1$ structures correspond to transitions between the top two valence bands and the lowest conduction band along the $\Lambda(<111>)$direction in the Brillouin zone. The $E_0'/E_0'+\Delta_0'$ feature corresponds to transitions at the Γ point between the top valence band and the second (spin-orbit split) conduction band (associated with *p*-antibonding states). The E_2 transition includes contributions from different regions of the band structure, especially points close to the Brillouin zone edges in the $<100>$ and $<110>$ directions.

Notice that the signal-to-noise ratio for the E_0 transition is poor. In three of our samples, $Ge_{0.98}Sn_{0.02}$, $Ge_{0.88}Sn_{0.12}$, and $Ge_{0.86}Sn_{0.14}$, the Savitzky-Golay procedure leads to unacceptable shape distortions when computing second derivates from point-by-point dielectric functions. Therefore, for these samples we compute the derivatives from the parametric Johs-Herzinger lineshape. Even though this approach involves the risk of systematic errors, as discussed above, we are confident that in our case the resulting critical point energies are reliable. We draw this conclusion from the fact that the Johs-Herzinger lineshape provides an excellent fit to $\varepsilon=\varepsilon_1+i\varepsilon_2$, and that in the case of the $Ge_{0.92}Sn_{0.08}$ sample the derivatives of the point-by-point fit and the parametric lineshape lead to exactly the same value for E_0. We have also verified that removing the E_0 critical point from the Johs-Herzinger lineshape worsens the fit of the ellipsometric angles considerably, indicating that E_0 does make a substantial and measurable contribution to the optical constants in this energy range. The photoreflectance technique, discussed below, is much more sensitive to the E_0 transition, and our photoreflectance results fully confirm our ellipsometric assignments.

The expressions used to analyze the second-derivative lineshapes are

$$\frac{d^2\varepsilon}{dE^2}=\frac{A_0e^{i\Phi_0}}{(E-E_0+i\Gamma_0)^{3/2}}, \tag{2}$$

for the infrared range, corresponding to a three-dimensional critical point, and

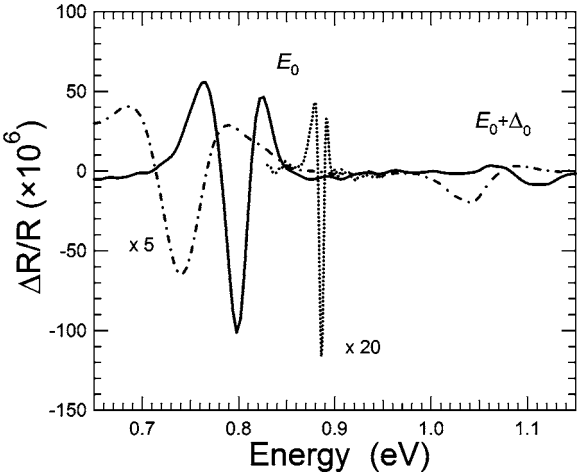

FIG. 6. Photoreflectance signal from Ge (dotted line). $Ge_{0.98}Sn_{0.02}$ (solid line) and $Ge_{0.96}Sn_{0.04}$ (dashed-dotted line). The data were collected at 15 K.

$$\frac{d^2\varepsilon}{dE^2} = \sum_j \frac{A_j e^{i\Phi_j}}{(E - E_j + i\Gamma_j)^2}, \tag{3}$$

for the visible range, where each term represents a two-dimensional critical point. The summation in Eq. (3) runs over all different transitions. A_j is the amplitude for transition j, E_j is the critical point energy, Γ_j is a phenomenological broadening, and Φ_j is a phase angle whose value is, in principle, determined by the geometrical nature of the critical point, but is taken as a free parameter to account for possible many-body effects. Equation (2) corresponds to a three-dimensional minimum in the electronic joint density of states, whereas Eq. (3) represents a mixture of a two-dimensional minimum and a saddle point. Both real and imaginary parts of Eq. (2) are fit simultaneously to the experimental data by a least-square procedure using a Levenberg-Marquardt algorithm.[58] Garland and coworkers (Ref. 59) have suggested an alternative procedure that eliminates any possible data distortion introduced by the numerical differentiation of the experimental dielectric function. Instead of fitting these numerical derivatives with analytical expressions such as those in Eqs. (2) and (3), they compute *numerical* derivatives of the model dielectric functions and fit those to the numerical derivatives of the experimental data. We have verified that in our case both approaches lead to virtually the same fit parameters. This is because lineshape distortions are severe mainly for sharp critical point features, whereas our critical points for alloy semiconductors at room temperature are relatively broad.

Since the $E_0'/E_0'+\Delta_0'$ doublet is not resolved (as is the case in pure Ge at room temperature[57]), it is modeled as a single critical point. All parameters in our fits are allowed to vary freely, except for the phase angles for the E_1 and $E_1+\Delta_1$ transitions, which are constrained to have the same value.

E. Photoreflectance measurements

Photoreflectance spectra were acquired using an automated photoreflectance system,[60] equipped for temperature ramping from 12 to 350 K. Data were collected over a spectral range of 0.55–1.15 eV with an energy resolution of 5 meV. The pump source was a 442 nm line from a He-Cd laser modulated at a frequency of 1 KhZ. The average power density of the pump source at the sample surface was 0.75 W/cm^2. The detector was a thermoelectrically cooled InGaAs photodiode.

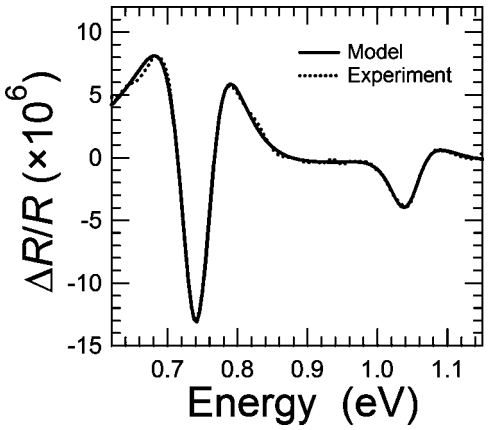

FIG. 7. Photoreflectance data (15 K) and fit with Eq. (4) and Eq. (5) for a $Ge_{0.96}Sn_{0.04}$ sample.

Most of our photoreflectance measurements were performed at 15 K. For one sample we also carried out measurements at room temperature for a comparison with the ellipsometric data. Figure 6 shows typical low-temperature results. The features observed correspond to the lowest direct band gap E_0 and to the $E_0+\Delta_0$ gap between the split-off Γ_7^v valence band and the same conduction band state as E_0. The E_0 transition is very strong in photoreflectance, in contrast with the ellipsometric measurements discussed above. The $E_0+\Delta_0$ transition is simply too weak to be observed with ellipsometry. Our results were analyzed using the lineshape functions

$$\frac{\Delta R}{R} = \mathrm{Re}\left(\frac{A_{\mathrm{ex}} e^{i\Phi_{\mathrm{ex}}}}{(E - E_{\mathrm{ex}} + i\Gamma_{\mathrm{ex}})^2} + \frac{A_0 e^{i\Phi_0}}{(E - E_0 + i\Gamma_0)^{5/2}} \right) + B_0 + C_0 E, \tag{4}$$

for the E_0 transition and

$$\frac{\Delta R}{R} = \mathrm{Re}\left(\frac{A_\Delta e^{i\Phi_\Delta}}{(E - E_\Delta + i\Gamma_\Delta)^{5/2}} \right) + B_\Delta E + C_\Delta, \tag{5}$$

for the $E_0+\Delta_0$ transition. Here $E_\Delta = E_0+\Delta_0$. These expressions are based on the assumption that photoreflectance is a third-derivative technique.[61] For the E_0 transition we include a three-dimensional critical point and the first derivative of a Lorentzian exciton, whereas the $E_0+\Delta_0$ transition is modeled with a single three-dimensional critical point. The linear background brings the fits to nearly perfect agreement with experiment, as seen in Fig. 7, but its removal has little effect on the energies and broadenings determined from the fits.

The nearly symmetric lineshape of the E_0 feature is a direct consequence of the electron-hole interaction. Without excitonic effects, the lineshape would be asymmetric, as found for the $E_0+\Delta_0$ transition. Notice that the E_0 lineshape

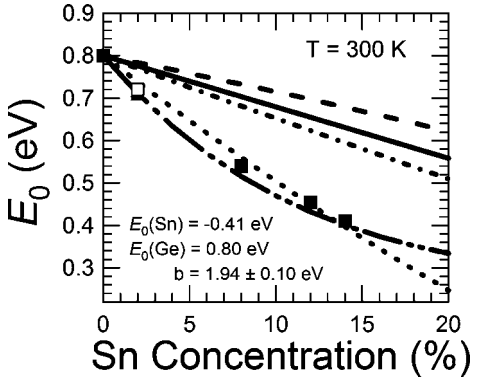

FIG. 8. Compositional dependence of the direct gap E_0 in $Ge_{1-y}Sn_y$ alloys at room temperature. The solid squares indicate band gaps obtained from ellipsometry; the empty square represents a photoreflectance measurement. The top dashed line represents a VCA pseudopotential calculation (Ref. 18). The solid line is a linear interpolation between Ge and α-Sn. The dashed-dotted line is a VCA calculation within a tight-binding formalism (Ref. 17). The dotted line is a fit with Eq. (1), and the dashed/double-dotted line is obtained using the compositional-dependent bowing proposed by Chibane *et al.* (Ref. 42).

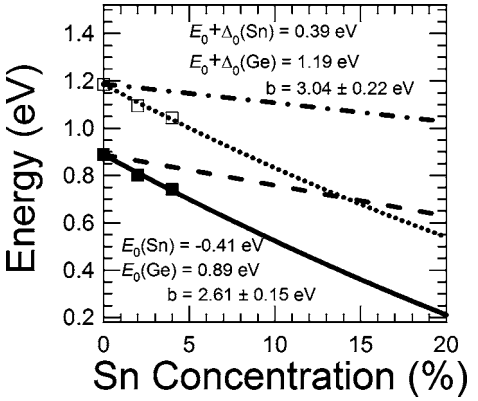

FIG. 9. Compositional dependence of the direct gap E_0 and the split-off gap $E_0+\Delta_0$ in $Ge_{1-y}Sn_y$ alloys at 15 K determined from photoreflectance measurements. The dashed-dotted and dashed lines are linear interpolations between Ge and α-Sn. The dotted and solid lines represent fits with Eq. (1). The bowing coefficients determined from these fits are affected by extrinsic strain effects, as discussed in the text.

is qualitatively similar in Ge and in the $Ge_{1-y}Sn_y$ samples, indicating that excitonic effects remain strong in the alloys. The exciton binding energy we obtain from the Ge fit is about 4.6 meV. This should be compared with a binding energy of 2 meV obtained from piezoreflectance by Yin *et al.*[62] The discrepancy is most likely due to the fact that we do not include a Sommerfeld enhancement factor in our expression for the three-dimensional minimum. We believe that our cruder approach is sufficient to study the compositional dependence of the band gap, but it is probably not fully adequate for a detailed study of excitonic binding energies. Therefore, we kept the exciton binding energy fixed at 4.6 meV for the $Ge_{1-y}Sn_y$ samples.

III. RESULTS AND COMPARISON WITH THEORY

Whenever possible, we have fit the compositional dependence of the critical point parameters with an expression equivalent to Eq. (1), using as end points the values we determined for Ge (very similar to previous work by Viña *et al.*[57]) and those for α-Sn from Ref. 63. Unless otherwise indicated, the end values were kept fixed, so that the fit has the bowing b as its only adjustable parameter. We find in all cases that a constant (compositionally independent) bowing provides an excellent fit to our data. This is consistent with similar measurements in $Ge_{1-x}Si_x$ alloys, which show no significant evidence for compositionally dependent bowing parameters.[29–32] It must be emphasized, however, that most of the $Ge_{1-x}Si_x$ measurements cover the entire compositional range, whereas our experimental data for $Ge_{1-y}Sn_y$ alloys are limited to a narrower range near the pure-Ge limit. Thus, we cannot rule out the possibility that some of the bowing parameters discussed here may be compositional dependent.

A. $E_0/E_0+\Delta_0$ transitions

1. E_0 transition

Figure 8 shows the compositional dependence of the direct gap from ellipsometric and photoreflectance measurements at room temperature. Figure 9 shows photoreflectance data for the same gap at 15 K. Notice that both techniques produce consistent results. The room temperature photoreflectance data point in Fig. 8 is in very good agreement with the ellipsometric data, and the relative energy shifts between the three low-temperature photoreflectance spectra are in good agreement with the relative shifts determined from ellipsometry.

It is apparent from Fig. 8 and Fig. 9 that the compositional dependence of E_0 deviates strongly from a linear interpolation between its values for pure Ge and $\alpha-$Sn. Notice that this linear interpolation uses a *negative* $E_0=-0.41$ eV for $\alpha-$Sn. In this material, the Γ_7 antibonding *s*-like level appears 0.41 eV *below* the *p*-type Γ_8 valence band edge.[64,65] In other words, the lowest conduction band state at Γ in Ge becomes a valence band in $\alpha-$Sn. The lowest conduction band in $\alpha-$Sn corresponds to the light-hole valence band in Ge, and the symmetry-imposed degeneracy of heavy and light holes at the center of the Brillouin zone implies that $\alpha-$Sn is a zero-gap semimetal.

The measured compositional dependence is fit with Eq. (1), yielding $b=1.94\pm0.1$ eV at room temperature and $b=2.61\pm0.15$ eV at a low temperature. We believe that the difference between the two measurements is largely due to the additional tensile strain on the $Ge_{1-y}Sn_y$ layers upon cooling to low temperatures (this is because the thermal expansion coefficient of Ge is larger than that of the Si substrate). The correction for this effect using the same band structure parameters as in Ref. 66 reduces the low-temperature bowing parameter to $b=2.26\pm0.09$ eV, in much better agreement with the room temperature measurements. The reason why a relatively small strain has a large effect on the bowing parameter fit is that we only have two low-temperature photoreflectance data points, and both points correspond to low Sn concentrations. By contrast, the room temperature data, which include more data points and extend up to 14% Sn, are very weakly affected by the residual com-

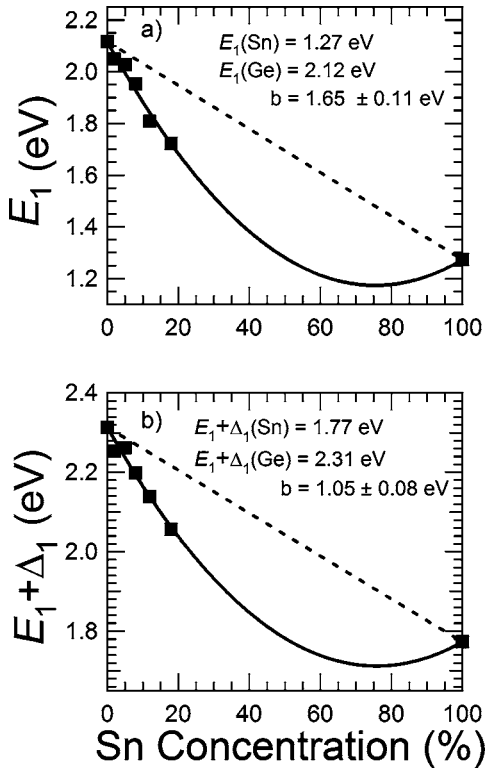

FIG. 10. Compositional dependence of the (a) E_1 and (b) $E_1+\Delta_1$ transition energies in $Ge_{1-y}Sn_y$ alloys.

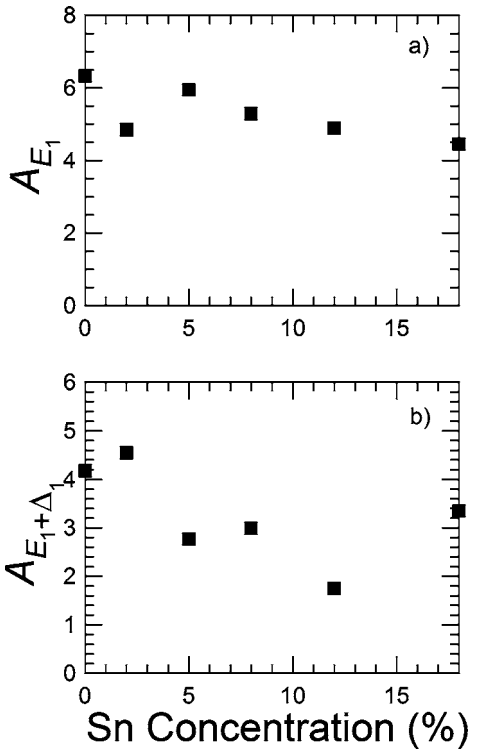

FIG. 11. Compositional dependence of the (a) E_1 and (b) $E_1+\Delta_1$ amplitude parameters in $Ge_{1-y}Sn_y$ alloys.

pressive strains measured by x rays, which are of comparable magnitude. An additional possible source of systematic errors in the bowing coefficient for the E_0 transition is the end point value for α-Sn. The negative $E_0=-0.41$ eV value was measured at low temperature, and it was found to be nearly temperature independent over the 1.5–85 K temperature range.[65] Here we assume $E_0=-0.41$ eV, even at room temperature, but we have verified that a shift as large as 0.1 eV would only change the bowing parameter by 0.04 eV, well within the experimental error of our fit.

The E_0 bowing obtained from our fits is smaller than the bowing $b=2.8$ eV reported by He and Atwater.[17] We believe that our determination is more accurate because we observe the E_0 gap directly, whereas in Ref. 17 E_0 is obtained from a fit to the optical absorption fit that includes the indirect gap and absorption by localized states.

The two theoretical calculations within the VCA predict a much smaller bowing: $b=-0.40$ eV for the pseudopotential approach[25] and $b=0.30$ for the tight-binding calculation.[24] This failure casts doubts on the predicted composition for a crossover from the indirect to the direct band gap. We discuss this point later. By contrast, a calculation by Chibane *et al.*[39] predicts a large, compositionally dependent bowing parameter that we have fit with the expression $b(y)=3.6-14y+17y^2$ eV for $y<0.5$. Using this expression, we compute the band gap shown as a double-dotted-dashed line in Fig. 8. The agreement with experiment is excellent. The method used by Chibane *et al.* is based on a structural model,[23] but few details are provided. The calculated bowing parameter is apparently obtained from the band gap difference between an ordered structure that simulates the random alloy and bulk Ge and α-Sn. The ordered structure is based on an 8-atom supercell, and no indication is given as to whether the alloy properties are sufficiently converged with such a small cell. The electronic structure is calculated using a standard density-functional approach (DFT) within the local-density approximation (LDA). To lowest-order, the well-known DFT-LDA band gap underestimation cancels out when computing bowing parameters from the band gap *difference* between two structures, but in the case of Ge the LDA band gap is vanishingly small,[67] and therefore it is not obvious that a DFT-LDA approach is valid. Since this issue is not addressed in Ref. 39, the impressive agreement with experiment should be taken with caution, although it strongly suggests that structural theories of bowing are superior to the VCA when it comes to the electronic structure of $Ge_{1-y}Sn_y$ alloys.

2. $E_0+\Delta_0$ transition

The ellipsometric measurements are not sensitive to the $E_0+\Delta_0$ transition, and therefore we must rely on the low-temperature photoreflectance data to obtain the compositional dependence of $E_0+\Delta_0$. The results are shown in Fig. 9. By comparing the $E_0+\Delta_0$ and E_0 bowings, it appears that the spin orbit splitting Δ_0 has a positive bowing. Unfortunately, the availability of only two $E_0+\Delta_0$ measurements for $Ge_{1-y}Sn_y$ alloys makes a determination very uncertain. Bowing parameters of spin-orbit splittings in $Ge_{1-y}Sn_y$ and $Ge_{1-x}Si_x$ alloys are discussed in detail in Sec. IV C.

3. E_1 and $E_1+\Delta_1$ transitions

In Fig. 10 we show the compositional dependence of the

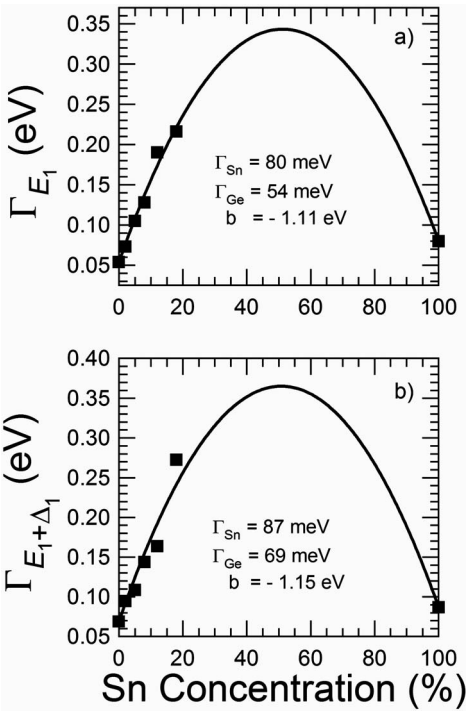

FIG. 12. Compositional dependence of the (a) E_1 and (b) $E_1+\Delta_1$ broadening parameters in $Ge_{1-y}Sn_y$ alloys.

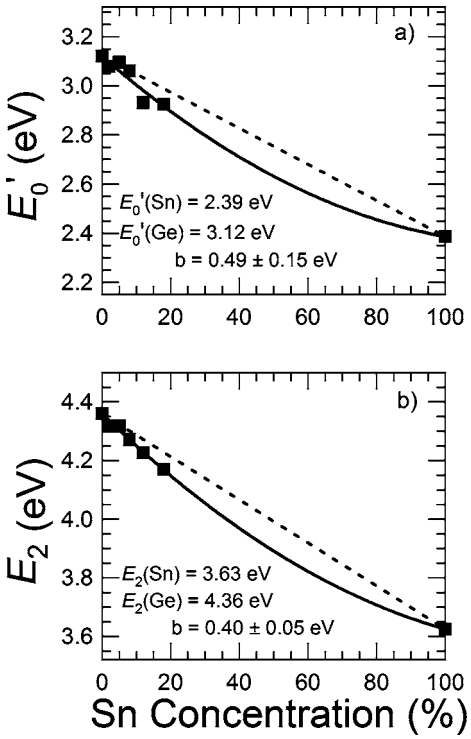

FIG. 13. Compositional dependence of the (a) E_0' and (b) E_2 transition energies in $Ge_{1-y}Sn_y$ alloys.

E_1 and $E_1+\Delta_1$ transitions in $Ge_{1-y}Sn_y$ alloys. Figure 11 and Fig. 12 show the evolution of the amplitudes and broadenings as a function of composition. A fit to the pseudopotential VCA calculation[25] gives a bowing $b=-0.17$ eV for the E_1 transition. Since this calculation does not include the spin-orbit interaction, it should be compared to the average of the experimental E_1 and $E_1+\Delta_1$ transitions. Experimentally, this average is $b=1.35$ eV, in strong disagreement with theory. Thus the E_1 transition results also suggest that the VCA is insufficient to describe $Ge_{1-y}Sn_y$ alloys. From a comparison of the bowings for the E_1 and $E_1+\Delta_1$ transitions we conclude that the spin-orbit splitting Δ_1 has a negative bowing. This is discussed in Sec. IV C.

It is interesting to note that the magnitude of the bowing for the E_1 and $E_1+\Delta_1$ transition energies is such that for high-Sn concentrations these transition energies are smaller than those in pure α-Sn. This explains the puzzling electroreflectance results of Oguz *et al.*,[9] who were the first to note this anomaly. For $y=0.78$, the Sn concentration in their sample, our fits predict $E_1=1.2$ eV and $E_1+\Delta_1=1.7$ eV, close to the measured values of 1.3 and 1.6 eV, respectively. The numerical agreement is very good, considering the fact that the sample in Ref. 9 is microcrystalline and its Sn concentration was obtained from x-ray data by assuming the validity of the Vegard' law.

B. E_0' and E_2 transitions

In Fig. 13 we show the compositional dependence of the E_0' and E_2 transitions in $Ge_{1-y}Sn_y$ alloys. From the fits with Eq. (1), we obtain bowing parameters $b=0.49$ eV (E_0') and $b=0.40$ eV (E_2). This should be contrasted with $b=0.22$ eV (E_0') and $b=-0.06$ eV (E_2) that we obtain from fitting the pseudopotential VCA calculation.[25] Again, we find that the agreement between experiment and theory is poor. In Fig. 14 we show the compositional dependence of the broadening for these transitions.

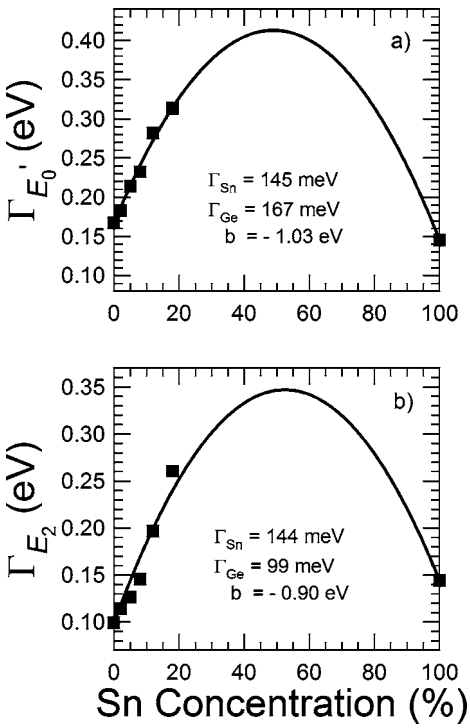

FIG. 14. Compositional dependence of the (a) E_0' and (b) E_2 broadening parameters in $Ge_{1-y}Sn_y$ alloys.

IV. COMPARISON WITH $Ge_{1-x}Si_x$ ALLOYS

A. Structural similarities between $Ge_{1-x}Si_x$ and $Ge_{1-y}Sn_y$ alloys

The phonon dispersion relations in pure Si, Ge, and α-Sn scale very well with the so-called "ionic-plasma frequencies."[68] Dimensionless ratios of elastic constants are very similar for the three materials. This suggests that the effective interatomic potentials that determine structural relaxations in $Ge_{1-x}Si_x$ alloys and $Ge_{1-y}Sn_y$ alloys are also similar and scalable. An important dimensionless quantity that characterizes structural relaxations in semiconductor alloy systems is the so-called topological rigidity parameter a^{**} defined by Cai and Thorpe.[69] (An equivalent structural relaxation parameter ε was defined by Martins and Zunger.[70]) This parameter relates the compositional dependence of bond lengths with the compositional dependence of the lattice constant: $\Delta d/d_0=(1-a^{**})(\Delta a/a_0)$. For $Ge_{1-x}Si_x$ alloys, first-principles theoretical calculations yield values of a^{**} between 0.6 (Ref. 71) to 0.7 (Ref. 72) for the Si-Si, Si-Ge, and Ge-Ge bonds. (A notable exception to the apparent unanimity of first-principles calculations is the recent work of Yu and co-workers.[73]) The experimental values of a^{**} for $Ge_{1-x}Si_x$ have been controversial, but the latest analysis of extended x-ray absorption (EXAFS) data indicate $a^{**}=0.6$ (Ref. 74). This value is supported by studies of the compositional dependence of Raman modes.[75] There are no experimental values of a^{**} for $Ge_{1-y}Sn_y$ alloys, but first-principles calculations[76] give $a^{**}=0.69$, similar to the $Ge_{1-x}Si_x$ results. The similarity between the two systems leads to a simple scaling relationship for the compositional dependence of Raman mode frequencies. This scaling has been verified experimentally.[46]

B. Review and reassessment of interband transitions in $Ge_{1-x}Si_x$ alloys

The analogous structural relaxation in $Ge_{1-x}Si_x$ and $Ge_{1-y}Sn_y$ alloys should lead to correlations between the electronic structures of the two alloy systems. In particular, bowing parameters for transition energies, broadenings, and spin-orbit splittings might follow a scaling behavior similar to that found for the vibrational properties. Unfortunately (and surprisingly), the relevant bowing parameters are not very well known in $Ge_{1-x}Si_x$ alloys, in spite of many years of intense research on this system. This is due to the fact that bowings in $Ge_{1-x}Si_x$ are small, and therefore very difficult to measure. In addition, the lowest direct gap E_0 at the center of the Brillouin zone is nearly impossible to detect in Si-rich $Ge_{1-x}Si_x$ alloys, because it sits very close in energy to the much stronger E_2 structure. To the best of our knowledge, the only available data for $E_0(x)$ are the room-temperature electro-reflectance measurements of Kline *et al.* (Ref. 29) for $x<0.5$ and the measurements of Aspnes and Studna for pure Si,[77] which yield $E_0=4.185\pm0.010$ eV and $E_0+\Delta_0=4.229\pm0.010$ eV at 4.2 K. If we take the temperature dependence of the direct band gap from the theoretical work of Lautenschlager *et al.* (Ref. 78), we estimate $E_0=4.093$ eV and $E_0+\Delta_0=4.137$ eV for Si at room temperature. Using

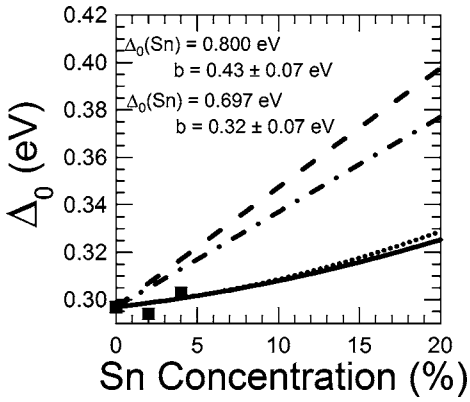

FIG. 15. Compositional dependence of the spin-orbit splitting Δ_0 in $Ge_{1-y}Sn_y$ alloys. The dashed and dashed-dotted lines represent two linear interpolations using different values for the spin-orbit splitting in α-Sn, as discussed in the text. The solid and dotted lines represent fits with Eq. (1) using each of those two end values for α-Sn.

$E_0=0.800$ eV as a fixed point, we fit the data of Ref. 29 and obtain a bowing parameter $b=0.21\pm0.04$ eV for the E_0 transition. Alternatively, if we do not force the E_0 fit to go through the $x=1$ value, we still obtain $b=0.17\pm0.1$ eV, but if we fit only the alloy data and discard the Si value completely, we obtain $b\sim0$. This underscores the need for more experimental work to confirm the $Ge_{1-x}Si_x$ bowing parameters.

For the $E_0+\Delta_0$ transition, Kline *et al.* have fewer data points measured at room temperature. Using those values and $E_0+\Delta_0=1.082$ eV (Ge); $E_0+\Delta_0=4.137$ eV (Si), we obtain a bowing parameter $b=0.14\pm0.06$ eV for the $E_0+\Delta_0$ transition.

The E_1 transition in $Ge_{1-x}Si_x$ alloys has been measured over the entire compositional range by Kline *et al.* (Ref. 29), Humlíček *et al.* (Ref. 30), Pickering *et al.* (Ref. 31), and Bahng *et al.* (Ref. 32). The $E_1+\Delta_1$ transition has been measured over the same range by Pickering *et al.* (Ref. 31) and Bahng *et al.* (Ref. 32). For E_1, the reported bowing parameters are $b=0.153$ eV (Refs. 30 and 31) and $b=0.27$ eV (Ref. 32). A fit of the data in (Ref. 29) with Eq. (1) gives $b=0.184\pm0.041$ eV. For $E_1+\Delta_1$, the two references that report measurements over the entire compositional range give $b=0.062$ eV (Ref. 31) and $b=0.065$ eV (Ref. 32). A larger bowing—$b=0.116\pm0.030$ eV—can be obtained from a fit to $E_1+\Delta_1$ data in Ref. 29, but these experiments only sample the $x<0.5$ range.

Even though there are non-negligible discrepancies between different measurements of $E_1/E_1+\Delta_1$, all studies indicate a negative bowing for the compositional dependence of the spin-orbit splitting Δ_1, consistent with the negative value we find for $Ge_{1-y}Sn_y$ alloys. This is discussed in depth in Sec. IV C.

For the E_0' transition, a fit to the data of Kline *et al.*[29] gives a vanishingly small bowing coefficient $b=-0.07\pm0.04$. Pickering *et al.* (Ref. 31) claim that their data are essentially linear as a function of composition, whereas Bahng *et al.* (Ref. 32) report a bowing coefficient $b=0.222$ eV. The E_2 transition has been analyzed as the combination of two critical points by Bahng *et al.*, (Ref. 32). The

TABLE I. Bowing parameters (in eV) for different optical interband transitions in $Ge_{1-x}Si_x$ and $Ge_{1-y}Sn_y$ alloys. The "Ratio" row shows the largest and smallest possible value computed from the data in the rows above. If these bowings were exactly proportional to the product of the size and electronegativity mismatch, the ratio of bowing parameters would be 0.083.

Alloy	E_0	$E_0+\Delta_0$	E_1	$E_1+\Delta_1$	E_0'	E_2
$Ge_{1-x}Si_x$	0.21[a,b]	0.14[a,b]	0.183[a]	0.116[a]	−0.07[a,b]	0.072[f]
			0.153[c,d]	0.062[d]	0[d]	0.084[g]
			0.27[e]	0.065[e]	0.22[e]	
$Ge_{1-y}Sn_y$	1.94[h]	3.04[i]	1.65[h]	1.05[h]	0.49[h]	0.4[h]
Ratio	0.11	0.046	0.09-0.16	0.06-0.11	0-0.45	0.18-0.21

[a]Reference 29.
[b]See the text for details on fits.
[c]Reference 30.
[d]Reference 31.
[e]Reference 32.
[f]Reference 32, fit to the $E_2(\Sigma)$ transition.
[g]Reference 32, fit to the $E_2(X)$ transition.
[h]Our work, room temperature.
[i]Our work, low temperature.

two transitions have bowing parameters $b=0.084$ eV and $b=0.072$ eV. The earlier data of Kline *et al.* (Ref. 29) are linear within experimental error.

The compositional dependence of the broadening parameters for $Ge_{1-x}Si_x$ alloys has also been studied by Bahng *et al.* (Ref. 32). A fit to those broadenings with an expression equivalent to Eq. (1) gives $b=-0.15$, -0.17, and -0.16 eV for E_1, $E_1+\Delta_1$, and E_0', respectively, and -0.07 eV/-0.10 eV for the two critical points associated with the E_2 transitions in this paper. Unfortunately, the broadening parameters are sensitive to the details of the procedure adopted to perform the numerical derivatives, as mentioned in Sec. II D, so that it is not straightforward to compare results from different authors. We note, for example, that the broadenings for pure Ge from Bahng *et al.* (Ref. 32) are substantially larger than our own values and those of Viña *et al.* (Ref. 57).

In Table I we summarize the bowing parameters for the compositional dependence of interband transition energies in $Ge_{1-x}Si_x$ and $Ge_{1-y}Sn_y$ alloys.

C. Comparison of spin-orbit splittings

1. Spin-orbit splitting Δ_0

The difference between the $E_0+\Delta_0$ and E_0 transitions measured with photoreflectance gives the spin-orbit splitting Δ_0. The results are shown in Fig. 15. The two experimental values are considerably below a linear interpolation between $\Delta_0=0.297\pm0.001$ eV for Ge (Ref. 79) and $\Delta_0=0.80^{+0.07}_{-0.04}$ eV for α-Sn, (Ref. 65) so that it appears that the bowing of the spin-orbit splitting Δ_0 is positive. A fit with an expression analogous to Eq. (1) gives $b=0.43\pm0.07$ eV. This value should be taken as very tentative, not only due to the very limited number of experimental points, but also because not even the α-Sn end value is known with great certainty. Groves *et al.* [65] determined this parameter from a $\boldsymbol{k}\cdot\boldsymbol{p}$ analysis of magnetoreflectance data. The authors note that the version of $\boldsymbol{k}\cdot\boldsymbol{p}$ theory used in their paper gives an overall excellent account of the data, but is unable to explain all experimental details. Depending on how the data is interpreted, the spin-orbit splitting could be as low as $\Delta_0=0.71$ eV. Interestingly, Brudevoll and co-workers have shown[80] that the near-band gap band structure of α-Sn obtained from first-principles calculations cannot be fit exactly with a $\boldsymbol{k}\cdot\boldsymbol{p}$ model similar to the one used by Groves *et al.* (Ref. 65) Brudevoll and co-workers predict[38,80] $\Delta_0=0.726$ eV for α-Sn and $\Delta_0=0.311$ eV for Ge, the latter very close to the experimental value $\Delta_0=0.297$ eV (Ref. 79). A more recent theoretical analysis of spin-orbit splittings in diamond and zincblende semiconductors,[81] predicts $\Delta_0=0.697$ eV for α-Sn, and $\Delta_0=0.302$ eV for Ge. For group IV semiconductors the calculated values are either in exact agreement with experiment or, with the exception of α-Sn, slightly larger than the experimental values. We also note that the ratio Δ_1/Δ_0 of spin-orbit splittings at the L and Γ points of the Brillouin zone in Ge is 0.67, in agreement with the so-called "two-thirds" rule.[82,83] From the measured $\Delta_1=0.50$ eV for α-Sn at room temperature, (Ref. 63) we would expect $\Delta_0=0.75$ eV if the same ratio is applicable to α-Sn. All these observations, combined, suggest that the Δ_0 value for α-Sn might be somewhat smaller than 0.80 eV. To see the possible impact of this alternative end value we fit the data in Fig. 15 using $\Delta_0=0.697$ eV for α-Sn. This gives a bowing parameter $b=0.32\pm0.07$ eV for $\Delta_0(x)$.

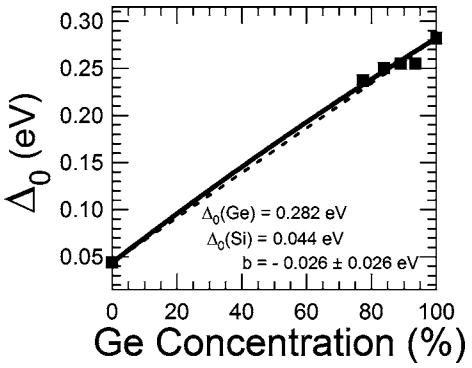

FIG. 16. Compositional dependence of the spin-orbit splitting Δ_0 in $Ge_{1-x}Si_x$ alloys from the electroreflectance data from Kline *et al.* (Ref. 32).

For $Ge_{1-x}Si_x$ alloys, we show in Fig. 16 the spin-orbit splitting that we obtain from the electroreflectance data of Kline *et al.* (Ref. 29) A fit of this quantity using the end values $\Delta_0=0.282$ eV for Ge (Ref. 29) and $\Delta_0=0.044$ eV for Si (Ref. 77), gives a bowing $b=-0.026\pm0.026$, that is, the spin-orbit splitting is a linear function of composition within experimental error.

The theory of Van Vechten *et al.* ascribes the positive bowing of $\Delta_0(x)$ observed in many semiconductors to s-p mixing in the valence band due to alloy potential fluctuations.[84] Van Vechten *et al.* and Hill,[85] propose expressions equivalent to

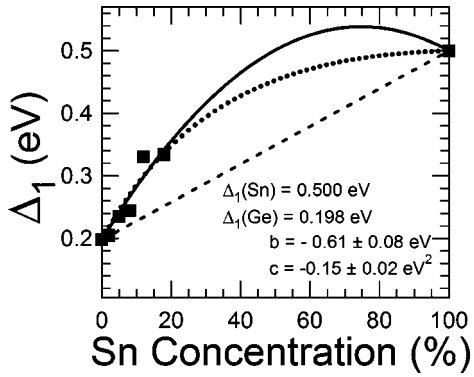

FIG. 17. Compositional dependence of the spin-orbit splitting Δ_1 in $Ge_{1-y}Sn_y$ alloys. The solid line represents a fit with an expression analog to Eq. (1). The dashed line is a linear interpolation between Ge and α-Sn, and the dotted line is calculated with an expression analog to Eq. (1), but using a compositional-dependent bowing parameter as given in Eq. (7).

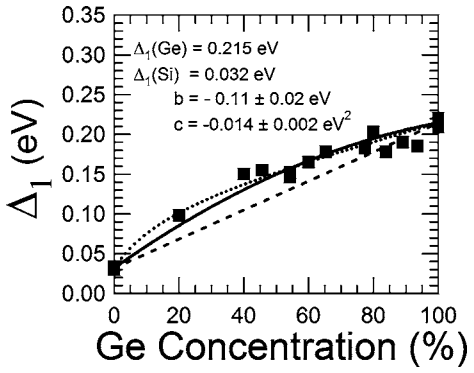

FIG. 18. Compositional dependence of the spin-orbit splitting Δ_1 in $Ge_{1-x}Si_x$ alloys. The experimental data has been collected from Kline *et al.* (Ref. 29) and Bahng *et al.* (Ref. 32) The solid line represents a fit with an expression analog to Eq. (1). The dashed line is a linear interpolation between Si and Ge, and the dotted line is calculated with an expression analog to Eq. (1) but using a compositional-dependent bowing parameter as given in Eq. (7).

$$\frac{b(\Delta_0)}{\Delta_{0L}(y)} = \frac{b(E_0)}{E_{0L}(y)}, \tag{6}$$

where $\Delta_{0L}(y)$ and $E_{0L}(y)$ are linear interpolations between the end values. Using perturbation theory, Chadi[83] also obtains an expression in which the bowing of Δ_0 is inversely proportional to an average band gap. Aside from the fact that the underlying theory has been questioned on the basis of first-principles calculations,[86] it is apparent that Eq. (6) cannot be valid for $Ge_{1-y}Sn_y$ alloys over the entire compositional range, because $E_{0L}(y)$ becomes zero. In terms of Chadi's perturbation treatment, one would need to use degenerate perturbation theory. Nevertheless, if we assume Eq. (6) to be valid for Ge rich alloys, we predict for our samples $b(\Delta_0) < 0.7b(E_0) = 0.7 \times 1.94$ eV $= 1.4$ eV. For $Ge_{1-x}Si_x$ alloys we predict $b(\Delta_0) < 0.3b(E_0) = 0.3 \times 0.21$ eV $= 0.06$ eV. The theory thus appears to justify the failure to observe any bowing in $\Delta_0(x)$ for $Ge_{1-x}Si_x$ alloys, and it is not inconsistent with our findings for $Ge_{1-y}Sn_y$ alloys. We insist, however, that the experimental uncertainty in the bowing of $\Delta_0(x)$ is too large to draw any definitive conclusions.

2. Spin-orbit splitting Δ_1

In Fig. 17 we show our measured Δ_1 values for $Ge_{1-y}Sn_y$ alloys, and in Fig. 18 we show values of Δ_1 in $Ge_{1-x}Si_x$ alloys obtained from two references[29,32] that present E_1 and $E_1+\Delta_1$ data in tabulated form. It is apparent that for both alloy systems the bowing of Δ_1 is negative. We also notice that the Δ_1 bowing is approximately proportional to the bowing of $\bar{E}_1 = E_1 + \Delta_1/2$, shown in Table II. This is the value of the E_1 transition in the absence of spin-orbit interaction. The ratio between these two quantities is -0.45 for $Ge_{1-y}Sn_y$ and somewhere between -0.70 and -1 for $Ge_{1-x}Si_x$. A stronger correlation between the two systems can be obtained if we assume a compositionally dependent bowing of the form

$$b(\Delta_1; y) = \frac{c}{\Delta_{1L}(y)}. \tag{7}$$

Fits with this bowing are shown as dotted lines in Fig. 17 and Fig. 18, and we see that the fit quality is as good (and perhaps even better in the case of $Ge_{1-x}Si_x$ alloys) than the fit with the standard constant bowing. The fit parameters are such that $c/b(\bar{E}_1)$ is -0.11 eV for $Ge_{1-y}Sn_y$ alloys and between -0.08 and 0.13 eV for $Ge_{1-x}Si_x$ alloys. Equation (7) can be obtained from a theory that assumes that the bowing in the spin orbit splitting is due to a disorder perturbation potential that couples the two spin-orbit split bands[84] Vishnubhata *et al.*[87] observed that in several *III-V* alloys the compositional dependence of the spin-orbit splitting Δ_1 is well reproduced by setting the bowing parameter equal to the difference between the end-point spin-orbit values. If this were to apply to $Ge_{1-y}Sn_y$ alloys as well, we should have $b = -0.3$ eV, a factor of 2 smaller than the experimental value.

3. Comparison of bowing parameters for interband transitions

It is apparent from Table I that the $Ge_{1-y}Sn_y$ bowings are larger than $Ge_{1-x}Si_x$ bowings by factors that range from 2 to

TABLE II. Bowing parameters (in eV) for the $\bar{E}_0$ and $\bar{E}_1$ optical transitions in $Ge_{1-x}Si_x$ and $Ge_{1-y}Sn_y$ alloys. These are calculated from the measured E_0 and E_1 transitions by subtracting the effect of the spin-orbit interaction. The "Ratio" row shows the largest and smallest possible value computed from the data in the rows above. If these bowings were exactly proportional to the product of the size and electronegativity mismatch, the ratio of bowing parameters would be 0.083.

Alloy	$\bar{E}_0$	$\bar{E}_1$
$Ge_{1-x}Si_x$	0.22[a,b]	0.11[c]
		0.17[d]
$Ge_{1-y}Sn_y$	2.08[e]	1.35[e]
Ratio	0.11	0.081–0.13

[a]Reference 29.
[b]See the text for details on fits.
[c]Reference 31.
[d]Reference 32.
[e]Our work.

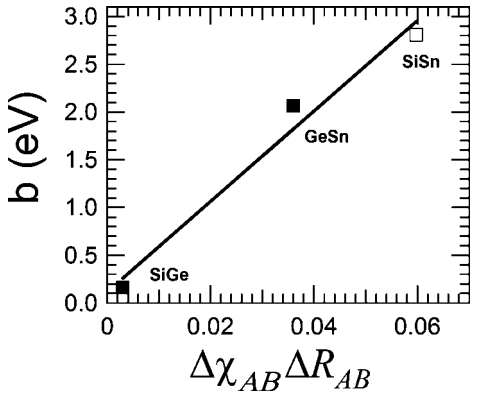

FIG. 19. Bowing parameters for the E_0 average gap in $Ge_{1-x}Si_x$, $Ge_{1-y}Sn_y$, and $Si_{1-z}Sn_z$ alloys. The $Ge_{1-x}Si_x$ and $Ge_{1-y}Sn_y$ data are experimental, the $Si_{1-z}Sn_z$ is from a theoretical calculation by Ferhat and Zaoui (Ref. 89).

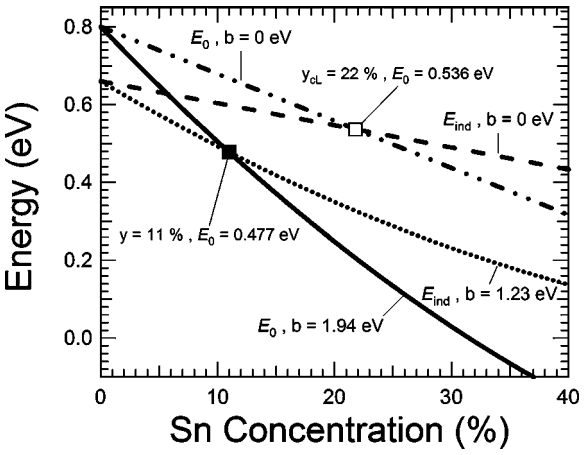

FIG. 20. Predicted compositional dependencies of the direct and indirect band gap in $Ge_{1-y}Sn_y$ alloys. The dashed-double-dotted and dashed lines represent linear interpolations between Ge and α-Sn. The solid line is our experimental result for the direct gap. The dotted line represents the indirect gap computed with b_{ind} =1.23 eV, which we believe is an upper limit for the value of this unknown bowing parameter. This means that the concentration y for the indirect to direct transition in $Ge_{1-y}Sn_y$ alloys should be less than 0.11.

17. Bernard and Zunger point out that their calculated bowings for a number of semiconductor alloys (which, unfortunately, do not include group IV alloys) scale with the product $\Delta\chi_{AB}\Delta R_{AB}$ of the electronegatively and atomic size mismatches.[23] If we use data from Phillips,[88] a similar scaling would lead to $Ge_{1-y}Sn_y$ bowings that are 12 times larger than $Ge_{1-x}Si_x$ bowings, within the range of the experimental observations. To study this in further detail, it is convenient to narrow down our comparison to transitions that are equivalent beyond doubt, and to separate purely band-structure effects from spin-orbit contributions, since the bowing for the band separations and the bowing for the spin-orbit splittings might have different physical origins. We note that the E_0' feature actually consists of two transitions, E_0' and $E_0'+\Delta_0'$, that are not resolved except in pure Ge at low temperatures[57] The very different values of the spin-orbit splittings in the two systems and the possibility that Δ_0' might have a significant bowing could introduce artifacts in a bowing comparison. In addition, the bowing for E_0' in $Ge_{1-x}Si_x$ alloys obtained by Bahng *et al.* (Ref. 32) is b=0.222 eV, while other authors claim that this transition's bowing is essentially zero. With this level of uncertainty we cannot draw any conclusion from comparing the bowing of E_0' in $Ge_{1-x}Si_x$ and $Ge_{1-y}Sn_y$. As to the E_2 transitions, they originate from different regions in the Brillouin zone of these semiconductors. The relative mix of $\boldsymbol{k}$-space contributions could easily change as a function of composition, and therefore we might be looking at different states when comparing E_2 in $Ge_{1-x}Si_x$ and $Ge_{1-y}Sn_y$ alloys. Because of these uncertainties, we limit any further comparison to the E_0 and E_1 transitions.

If there were no spin-orbit splittings, the measured E_0 and E_1 transition energies would be $\bar{E}_0=E_0+\Delta_0/3$ and $\bar{E}_1=E_1+\Delta_1/2$. In Table II we show the bowings for these two energies. We see that for $\bar{E}_0$ the ratio of bowing parameters is between 0.077, whereas for $\bar{E}_1$ the ratio of bowing parameters is between 0.08 and 0.13. These values are close to the ratio 0.083 expected if the bowing parameters are proportional to $\Delta\chi_{AB}\,\Delta R_{AB}$. In Fig. 19 we show the bowings for $\bar{E}_0=E_0+\Delta_0/3$ for $Ge_{1-y}Sn_y$ and $Ge_{1-x}Si_x$ alloys as a function of $\Delta\chi_{AB}\Delta R_{AB}$. We see that the bowings follow a straight line with a nearly zero intercept. The figure also includes the predicted bowing for $Si_{1-z}Sn_z$ alloys,[89]which is remarkably close to the extrapolation from the experimental $Ge_{1-x}Si_x$ and $Ge_{1-y}Sn_y$ values.

4. Comparison of bowing parameters for broadenings

The experimental bowing parameters for the E_1, $E_1+\Delta_1$, E_0', and E_2 transitions in $Ge_{1-y}Sn_y$ alloys are all similar, ranging from −0.90 to −1.15 eV. Interestingly, we find the same behavior for the E_1, $E_1+\Delta_1$, E_0' transitions in $Ge_{1-x}Si_x$ alloys, which range from −0.1 to −0.17 eV. (The E_2 transition has been fit with two critical points in $Ge_{1-x}Si_x$ alloys,[32] and therefore it cannot be compared directly to our E_2 fits in $Ge_{1-y}Sn_y$alloys.) The ratio between bowing parameters in the two systems is about 0.1, that is, it is comparable to the ratio of bowing parameters for the transition energies. This correlation between critical point broadenings and energies suggest that structural effects control the behavior of both types of parameters.

V. IMPLICATIONS FOR THE DIRECT-INDIRECT CROSSOVER

The two VCA calculations of the band structure of $Ge_{1-y}Sn_y$ alloys predict that the band gap becomes direct for $0.2\geqslant y_{c,\text{VCA}}\leqslant 0.26$. This is very close to the value y_{cL} =0.22 obtained from a simple linear interpolation between Ge and α-Sn, shown in Fig. 20. However, our observation of strong nonlinearities in the compositional dependence of all interband transitions casts serious doubts on the accuracy of the theoretically predicted $y_{c,\text{VCA}}$. Using absorption measurements, He and Atwater,[17] and Pérez Ladrón de Guevara *et al.*[19] determine a crossover concentration $y_c\sim 0.1$, well be-

low the VCA prediction. Unfortunately, the reliability of such measurements is hard to establish, since in Ge the indirect gap absorption is about two orders of magnitude weaker than the direct gap absorption. Thus, any alloy broadening of the direct gap could overlap the indirect absorption. Moreover, in order to fit their data these authors had to introduce a third contribution from localized states, which were associated with dislocations. This further increases the uncertainty of the absorption edge determination. It is important to point out that our ellipsometric and photoreflectance data can be understood in terms of a broadened direct transition. In our samples we find no evidence for the indirect edge or for absorption by localized states.

The indirect gap E_{ind} in a semiconductor with a Ge-like band structure is given by

$$E_{\mathrm{ind}} = \bar{E}_1 + E(L_{3v}) - \frac{\Delta_0}{3}, \tag{8}$$

where $\bar{E}_1$ is defined above and $E(L_{3v})$ is the energy of the highest valence band at the L point of the Brillouin zone (in the absence of spin-orbit coupling) measured with respect to the maximum of the valence band at the Γ point in the absence of spin-orbit coupling ($\Gamma_{25'}$ state; see, for example, Ref. 54). As a consequence of Eq. (8), $b(E_{\mathrm{ind}})=b(\bar{E}_1)+b(L_{3v})-b(\Delta_0)/3$. If $b(E_{\mathrm{ind}})<b(E_0)$, then $y_c<y_{cL}\sim y_{c,\mathrm{VCA}}$. For our $Ge_{1-y}Sn_y$ alloys, $b(\bar{E}_1)-b(\Delta_0)/3=1.21$ eV and $b(E_0)=1.94$ eV. Therefore, $y_c<y_{cL}\sim y_{c,\mathrm{VCA}}$ if $b(L_{3v})<0.7$ eV. The bowing $b(L_{3v})$ is not known experimentally, but calculations of this parameter for several *II-VI* and *III-V* alloys semiconductors show that it is *negative*.[36] The same appears to be valid for group IV alloys. The CPA calculations[27,90] of Krishnamurty *et al.*, give $b(L_{3v})=-0.11$ eV. These calculations overestimate the experimental band gap bowings, but given their overall agreement with experiment, it is unlikely that the *sign* of $b(L_{3v})$ will be incorrect. In tight-binding theory,[44] $E(L_{3v})$-$E(\Gamma_{25'})=2V_{pp\pi}=-1.2\,\hbar^2/(md^2)$ for a homopolar semiconductor. (Here d is the interatomic distance. All notation is from Harrison.[44]) The d^{-2} dependence means that the VCA contribution to the bowing of $E(L_{3v})$-$E(\Gamma_{25'})$ is negative, so that it is not entirely surprising that calculations incorporating effects beyond the VCA still show $b(L_{3v})<0$. The very important implication for our $Ge_{1-y}Sn_y$ work is that the crossover composition y_c should be smaller than previously assumed. We can obtain an upper limit for y_c by assuming $b(L_{3v})=0$. In this case, the indirect gap would be given by the dotted line in Fig. 20, and the crossover occurs for $y=0.11$. Therefore, $y_c\leqslant 0.11$. This is, interestingly, in agreement with Refs. 17 and 19.

A remarkable property of the bowing parameters $b(L_{3v})$ computed by Wei and Zunger[36] is that they are approximately proportional to the product of the electronegativity and atomic size mismatches. If the same scaling behavior were valid for $Ge_{1-y}Sn_y$ and $Ge_{1-x}Si_x$ alloys, we could *predict* $b(L_{3v})$ [and therefore, from Eq. (8), $b(E_{\mathrm{ind}})$] for $Ge_{1-y}Sn_y$ alloys from its value for $Ge_{1-x}Si_x$ alloys. The procedure involves three steps: (i) use the *known* $b(E_{\mathrm{ind}})$ and Eq. (8) to obtain $b(L_{3v})$ in $Ge_{1-x}Si_x$; (ii) multiply the resulting $b(L_{3v})$ by the appropriate scaling factor to obtain its value in $Ge_{1-y}Sn_y$; and (iii) apply Eq. (8) again in a reverse direction to obtain $b(E_{\mathrm{ind}})$ for $Ge_{1-y}Sn_y$. Unfortunately, since the scaling factor is 12, any error in $b(L_{3v})$ for $Ge_{1-x}Si_x$ alloys would be severely magnified when computing the same parameter for $Ge_{1-y}Sn_y$ alloys. The experimental data of Weber and Alonso,[91] and Morar and Batson[92] implies that for $Ge_{1-x}Si_x$ alloys the bowing of the indirect gap a the L point is $b(E_{\mathrm{ind}})\sim 0$. Moreover, since $b(\Delta_0)\sim 0$ in this system, we obtain $b(L_{3v})=-b(\bar{E}_1)$. Thus, from Table II, $b(L_{3v})<0$. This is in agreement with the theoretical arguments discussed previously. If we take $b(\bar{E}_1)=0.11$ eV from Table II, then $b(L_{3v})=-0.11$ eV, which, intriguingly, is in exact agreement with the theoretical prediction from the CPA calculations[27,90] of Krishnamurty *et al.* that we discussed previously. From our scaling argument we expect $b(L_{3v})=-1.32$ eV for $Ge_{1-y}Sn_y$ alloys, leading to [Eq. (8)] $b(E_{\mathrm{ind}})=-0.11$ eV. The indirect gap calculated with this bowing is almost indistinguishable from the linear interpolation, shown as a dashed line in Fig. 20, so that y_c could be as low as $y_c=0.06$. In fact, the crossover composition would be even smaller if we had based our scaling argument on the value $b(\bar{E}_1)=0.17$ eV for $Ge_{1-x}Si_x$ from the work of Bahng *et al.*[32] We insist, however, that the error in these predictions is very large, not only because of the large scaling factor from $Ge_{1-x}Si_x$ to $Ge_{1-y}Sn_y$ alloys, but also because our calculated $b(E_{\mathrm{ind}})$ for $Ge_{1-y}Sn_y$ alloys turns out to be given by the difference between two larger numbers. Photoluminescence experiments to locate the crossover concentration y_c are currently underway.

VI. CONCLUSIONS

An in-depth comparison of the electronic structure of $Ge_{1-y}Sn_y$ and $Ge_{1-x}Si_x$ reveals intriguing correlations. Although fraught with considerable experimental uncertainty, these correlations suggest a scaling behavior between bowing parameters in $Ge_{1-y}Sn_y$ and $Ge_{1-x}Si_x$ alloys. This scaling is not only interesting from a theoretical perspective, but it has practical implications. It is very unlikely that any correlation would exist if the wave functions for the corresponding conduction and valence band states in both alloy systems were too different. This is in strong contrast with $Si_{1-x}C_x$ alloys, where a localized level around C atoms either forms a lowest conduction band or lies just above it[93,94] We speculated in the Introduction that localized levels were unlikely in the $Ge_{1-y}Sn_y$ system. Our experimental results appear to be consistent with this initial presumption.

In addition to interband energies and broadenings, ellipsometry provides information on other critical point parameters, such as amplitudes and phases, that we have not discussed because there are no theoretical predictions. This underscores the limitations of current theories of alloy semiconductors. Calculations of the alloy dielectric function are rare (see, for example, Ref. 95) and the few authors who present such calculations do not compute the derivatives that would yield theoretically predicted amplitudes and phases. The latter, in particular, are strongly affected by excitonic effects, and we hope that recent successes in incorporating such effects into first-principles calculations of elemental and

compound semiconductors[96,97] will stimulate work on first-principles dielectric functions for alloy semiconductors.

ACKNOWLEDGMENTS

This work was supported by the National Science Foundation under Grant No. NSF-DMR-0221993, by the U.S. Air Force under Contract AFRL/SNHC (F19628-03-C-0056), by a grant from the Intel Corporation, and by the National Institute of Standards and Technology Contract No. 60NANB4D113. The infrared ellipsometer was purchased with a grant from the National Science Foundation, NSF-DMR-0315760.

[1] R. F. C. Farrow, D. S. Robertson, G. M. Williams, A. G. Cullis, G. R. Jones, I. M. Young, and M. J. Dennis, J. Cryst. Growth **54**, 507 (1981).
[2] S. I. Shah, J. E. Greene, L. L. Abels, Q. Yao, and P. M. Raccah, J. Cryst. Growth **83**, 3 (1987).
[3] M. T. Asom, E. A. Fitzgerald, A. R. Kortan, B. Spear, and L. C. Kimerling, Appl. Phys. Lett. **55**, 578 (1989).
[4] P. R. Pukite, A. Harwit, and S. S. Iyer, Appl. Phys. Lett. **54**, 2142 (1989).
[5] J. R. C. Bowman, P. M. Adams, M. A. Engelhardt, and H. Höchst, J. Vac. Sci. Technol. A **8**, 1577 (1990).
[6] J. Piao, R. Beresford, T. Licata, W. I. Wang, and H. Homma, J. Vac. Sci. Technol. B **8**, 221 (1990).
[7] O. Gurdal, M.-A. Hasan, J. M. R. Sardela, J. E. Greene, H. H. Radamson, J. E. Sundgren, and G. V. Hansson, Appl. Phys. Lett. **67**, 956 (1995).
[8] G. He and H. A. Atwater, Appl. Phys. Lett. **68**, 664 (1996).
[9] S. Oguz, W. Paul, T. F. Deutsch, B.-Y. Tsaur, and D. V. Murphy, Appl. Phys. Lett. **43**, 848 (1983).
[10] K. Ishida, H. Myoren, M. Yamamoto, T. Imura, and Y. Osaka, Jpn. J. Appl. Phys., Part 2 **28**, L125 (1989).
[11] H. Pérez Ladrón de Guevara, A. G. Rodríguez, H. Navarro-Contreras, and M. A. Vidal, Appl. Phys. Lett. **83**, 4942 (2003).
[12] M. Bauer, J. Taraci, J. Tolle, A. V. G. Chizmeshya, S. Zollner, D. J. Smith, J. Menendez, C. Hu, and J. Kouvetakis, Appl. Phys. Lett. **81**, 2992 (2002).
[13] M. R. Bauer, C. S. Cook, P. Aella, J. Tolle, J. Kouvetakis, P. A. Crozier, A. V. G. Chizmeshya, D. J. Smith, and S. Zollner, Appl. Phys. Lett. **83**, 3489 (2003).
[14] M. R. Bauer, J. Tolle, C. Bungay, A. V. G. Chizmeshya, D. J. Smith, J. Menendez, and J. Kouvetakis, Solid State Commun. **127**, 355 (2003).
[15] M. Bauer, C. Ritter, P. A. Crozier, J. Ren, J. Menendez, G. Wolf, and J. Kouvetakis, Appl. Phys. Lett. **83**, 2163 (2003).
[16] P. Aella, C. Cook, J. Tolle, S. Zollner, A. V. G. Chizmeshya, and J. Kouvetakis, Appl. Phys. Lett. **84**, 888 (2004).
[17] G. He and H. A. Atwater, Phys. Rev. Lett. **79**, 1937 (1997).
[18] R. Ragan and H. A. Atwater, Appl. Phys. Lett. **77**, 3418 (2000).
[19] H. Perez Ladron de Guevara, A. G. Rodriguez, H. Navarro-Contreras, and M. A. Vidal, Appl. Phys. Lett. **84**, 4532 (2004).
[20] C. S. Cook, S. Zollner, M. R. Bauer, P. Aella, J. Kouvetakis, and J. Menéndez, Thin Solid Films **455-456**, 217 (2004).
[21] M. L. Cohen and J. R. Chelikowsky, *Electronic Structure and Optical Properties of Semiconductors* (Springer-Verlag, Heidelberg, 1989).
[22] M. Jaros, Rep. Prog. Phys. **48**, 1091 (1985).
[23] J. E. Bernard and A. Zunger, Phys. Rev. B **36**, 3199 (1987).
[24] D. W. Jenkins and J. D. Dow, Phys. Rev. B **36**, 7994 (1987).
[25] K. A. Mäder, A. Baldereschi, and H. von Kanel, Solid State Commun. **69**, 1123 (1989).
[26] D. Stroud and H. Ehrenreich, Phys. Rev. B **2**, 3197 (1970).
[27] S. Krishnamurthy, A. Sher, and A. B. Chen, Phys. Rev. B **33**, 1026 (1986).
[28] K. E. Newman and J. D. Dow, Phys. Rev. B **30**, 1929 (1984).
[29] J. S. Kline, F. H. Pollak, and M. Cardona, Helv. Phys. Acta **41**, 968 (1968).
[30] J. Humlíček, M. Garriga, M. I. Alonso, and M. Cardona, J. Appl. Phys. **65**, 2827 (1989).
[31] C. Pickering, R. T. Carline, D. J. Robbins, W. Y. Leong, S. J. Barnett, A. D. Pitt, and A. G. Cullis, J. Appl. Phys. **73**, 239 (1993).
[32] J. H. Bahng, K. J. Kim, S. H. Ihm, J. Y. Kim, and H. L. Park, J. Phys.: Condens. Matter **13**, 777 (2001).
[33] J. Humlíček and M. Garriga, in *Silicon-Germanium Carbon Alloys*, edited by S. T. Pantelides and S. Zollner (Taylor and Francis, New York, 2002), Vol. 15, p. 483.
[34] J. D. D. Connolly and A. R. Williams, Phys. Rev. B **27**, 5169 (1983).
[35] A. Zunger, S.-H. Wei, L. G. Ferreira, and J. E. Bernard, Phys. Rev. Lett. **65**, 353 (1990).
[36] S.-H. Wei, L. G. Ferreira, J. E. Bernard, and A. Zunger, Phys. Rev. B **42**, 9622 (1990).
[37] F. Tekia, M. Ferhat, and Z. Zaoui, Physica B **293**, 183 (2000).
[38] T. Brudevoll, D. S. Citrin, N. E. Christensen, and M. Cardona, Phys. Rev. B **48**, 17128 (1993).
[39] Y. Chibane, B. Bouhafs, and M. Ferhat, Phys. Status Solidi B **240**, 116 (2003).
[40] S. H. Wei and A. Zunger, Phys. Rev. Lett. **76**, 664 (1996).
[41] A. St. Amour, C. W. Liu, J. C. Sturm, Y. Lacroix, and M. L. Thewalt, Appl. Phys. Lett. **67**, 3915 (1995).
[42] K. Brunner, K. Eberl, and W. Winter, Phys. Rev. Lett. **76**, 303 (1996).
[43] J. D. Lorentzen, G. H. Loechelt, M. Meléndez-Lira, J. Menéndez, S. Sego, R. J. Culbertson, W. Windl, O. F. Sankey, A. E. Bair, and T. L. Alford, Appl. Phys. Lett. **70**, 2353 (1997).
[44] W. A. Harrison, *Elementary Electronic Structure* (World Scientific, Singapore, 1999).
[45] W. G. Bi and C. W. Tu, Appl. Phys. Lett. **70**, 1608 (1997).
[46] S. F. Li, M. R. Bauer, J. Menéndez, and J. Kouvetakis, Appl. Phys. Lett. **84**, 867 (2004).
[47] J. P. Dismukes, L. Ekstrom, and R. J. Paff, J. Phys. Chem. **68**, 3021 (1964).
[48] A. V. G. Chizmeshya, M. R. Bauer, and J. Kouvetakis, Chem. Mater. **15**, 2511 (2003).
[49] C. M. Herzinger, B. Johs, W. A. McGahan, J. A. Woollam, and W. Paulson, J. Appl. Phys. **83**, 3323 (1998).
[50] T. E. Tiwald, D. W. Thompson, and J. A. Woollam, AVS, 1998, Vol. 16, p. 312.

[51] G. G. Devyatykh, E. M. Dianov, N. S. Karpychev, S. M. Mazavin, V. M. Mashinskii, V. B. Neustruev, A. V. Nikolaichik, A. M. Prokhorov, A. I. Ritus, N. I. Sokolov, and A. S. Yushin, Sov. J. Quantum Electron. **10**, 900 (1980).
[52] B. Johs, C. M. Herzinger, J. H. Dinan, A. Cornfeld, and J. D. Benson, Thin Solid Films **313-314**, 137 (1998).
[53] C. C. Kim, J. W. Garland, H. Abad, and P. M. Raccah, Phys. Rev. B **45**, 11749 (1992).
[54] P. Y. Yu and M. Cardona, *Fundamentals of Semiconductors: Physics and Materials Properties* (Springer-Verlag, Berlin, 1996).
[55] A. Savitzky and M. J. E. Golay, Anal. Chem. **36**, 1627 (1964).
[56] J. Steiner, Y. Termonia, and J. Deltour, Anal. Chem. **44**, 1906 (1972).
[57] L. Viña, S. Logothetidis, and M. Cardona, Phys. Rev. B **30**, 1979 (1984).
[58] W. H. Press, S. A. Teukolsky, W. T. Vetterling, and B. P. Flannery, *Numerical Recipes in C: The Art of Scientific Computing* (Cambridge University Press, New York, 1992).
[59] J. W. Garland, C. Kim, H. Abad, and P. M. Raccah, Phys. Rev. B **41**, 7602 (1990).
[60] F. Pollak, in *Handbook of Semiconductors: Optical Properties of Semiconductors*, edited by M. Balkanski (North-Holland, Amsterdam, 1994), Vol. 2, p. 527.
[61] D. E. Aspnes, Surf. Sci. **37**, 418 (1973).
[62] Y. Yin, D. Yan, F. H. Pollak, M. S. Hybertsen, J. M. Vandenberg, and J. C. Bean, Phys. Rev. B **52**, 8951 (1995).
[63] L. Viña, H. Höchst, and M. Cardona, Phys. Rev. B **31**, 958 (1985).
[64] S. Groves and W. Paul, Phys. Rev. Lett. **11**, 194 (1963).
[65] S. H. Groves and C. R. Pidgeon, J. Phys. Chem. Solids **31**, 2031 (1970).
[66] J. Menendez and J. Kouvetakis, Appl. Phys. Lett. **85**, 1175 (2004).
[67] M. S. Hybertsen and S. G. Louie, Phys. Rev. B **34**, 5390 (1986).
[68] W. Weber, Phys. Rev. B **15**, 4789 (1977).
[69] Y. Cai and M. F. Thorpe, Phys. Rev. B **46**, 15872 (1992).
[70] J. L. Martins and A. Zunger, Phys. Rev. B **30**, 6217 (1984).
[71] A. Qteish and R. Resta, Phys. Rev. B **37**, 1308 (1988).
[72] S. d. Gironcoli, P. Giannozzi, and S. Baroni, Phys. Rev. Lett. **66**, 2116 (1991).
[73] M. Yu, C. S. Jayanthi, D. A. Drabold, and S. Y. Wu, Phys. Rev. B **64**, 165205 (2001).
[74] D. B. Aldrich, R. J. Nemanich, and D. E. Sayers, Phys. Rev. B **50**, 15026 (1994).
[75] M. Meléndez-Lira, J. Menéndez, W. Windl, O. F. Sankey, G. S. Spencer, S. Sego, R. B. Culbertson, A. E. Bair, and T. L. Alford, Phys. Rev. B **54**, 12866 (1997).
[76] J. Shen, J. Zi, X. Xie, and P. Jiang, Phys. Rev. B **56**, 12084 (1997).
[77] D. E. Aspnes and A. A. Studna, Solid State Commun. **11**, 1375 (1972).
[78] P. Lautenschlager, P. B. Allen, and M. Cardona, Phys. Rev. B **31**, 2163 (1985).
[79] D. E. Aspnes, Phys. Rev. B **12**, 2297 (1975).
[80] T. Brudevoll, D. S. Citrin, M. Cardona, and N. E. Christensen, Phys. Rev. B **48**, 8629 (1993).
[81] P. Carrier and S.-H. Wei, Phys. Rev. B **70**, 035212 (2004).
[82] M. Cardona, *Modulation Spectroscopy* (Academic, New York, 1969).
[83] D. J. Chadi, Phys. Rev. B **16**, 790 (1977).
[84] J. A. Van Vechten, O. Berolo, and J. C. Woolley, Phys. Rev. Lett. **29**, 1400 (1972).
[85] R. Hill, J. Phys. C **7**, 516 (1974).
[86] S.-H. Wei and A. Zunger, Phys. Rev. B **39**, 6279 (1989).
[87] S. S. Vishnubhata, B. Eyglunent, and J. C. Woolley, Can. J. Phys. **47**, 1661 (1969).
[88] J. C. Phillips, *Bonds and Bands in Semiconductors* (Academic, New York, 1973).
[89] M. Ferhat and A. Zaoui, Infrared Phys. Technol. **42**, 81 (2001).
[90] S. Krishnamurthy, A. Sher, and A.-B. Chen, Appl. Phys. Lett. **47**, 160 (1985).
[91] J. Weber and M. I. Alonso, Phys. Rev. B **40**, 5683 (1989).
[92] J. F. Morar and P. E. Batson, J. Vac. Sci. Technol. B **10**, 2022 (1992).
[93] A. A. Demkov and O. F. Sankey, Phys. Rev. B **48**, 2207 (1993).
[94] W. Windl, A. A. Demkov, and O. F. Sankey, in *Silicon-Germanium Carbon Alloys: Growth, Properties, and Applications*, edited by S. T. Pantelides and S. Zollner (Taylor & Francis, New York, 2002), Vol. 15, p. 237.
[95] G. Theodorou, G. Tsegas, P. C. Kelires, and E. Kaxiras, Phys. Rev. B **60**, 11494 (1999).
[96] L. X. Benedict, E. L. Shirley, and R. B. Bohn, Phys. Rev. B **57**, R9385 (1998).
[97] M. Rohlfing and S. G. Louie, Phys. Rev. B **62**, 4927 (2000).